Obstetrics & Gynaecology Publications   Obstetrics & Gynaecology Department

7-6-2016

P66Shc, a key regulator of metabolism and mitochondrial ROS production, is dysregulated by mouse embryo culture.

Nicole A Edwards

Andrew J Watson

Dean H Betts

Follow this and additional works at: https://ir.lib.uwo.ca/obsgynpub

 Part of the Obstetrics and Gynecology Commons

OXFORD UNIVERSITY PRESS | Molecular Human Reproduction

P66Shc, a key regulator of metabolism and mitochondrial ROS production, is dysregulated by mouse embryo culture

Journal:	*Molecular Human Reproduction*
Manuscript ID	Draft
Manuscript Type:	Original Research
Date Submitted by the Author:	n/a
Complete List of Authors:	nedwar@uwo.ca, Nicole; Western University, Physiology and Pharmacology Watson, Andy; Western University, Physiology and Pharmacology Betts, Dean; University of Western Ontario, Physiology & Pharmacology
Key Words:	blastocyst, cell culture, embryology, gene expression, metabolism

SCHOLARONE™
Manuscripts

1 **P66Shc, a key regulator of metabolism and mitochondrial ROS production, is**

2 **dysregulated by mouse embryo culture**

3

4 Running title: p66Shc in preimplantation mouse embryos

5

6 Nicole A. Edwards[1], Andrew J. Watson[1,2,3], Dean H. Betts[1,2,3,*]

7 [1]Departments of Physiology and Pharmacology, and [2]Obstetrics and Gynaecology, Schulich

8 School of Medicine & Dentistry, The University of Western Ontario; [3]The Children's Health

9 Research Institute (CHRI), Lawson Health Research Institute, London, Ontario, Canada. N6A

10 5C1

11
12 [*]Corresponding author:
13
14 Dean H. Betts:
15 Tel: +1-519-661-2111 ext. 83786;
16 E-mail: dean.betts@schulich.uwo.ca

Abstract

17   **Study hypothesis:** High oxygen tension and high medium glucose concentrations dysregulate

18   p66Shc expression and function during mouse preimplantation embryo culture.

20   **Study finding:** P66Shc expression abnormally increases and oxidative phosphorylation

21   metabolism is impaired in blastocysts produced in culture.

22   **What is known already:** Growth in culture adversely impacts preimplantation embryo

23   development and alters the expression levels of the oxidative stress adaptor protein p66Shc, but

24   it is not known if p66Shc expression differences are linked to metabolic changes observed in

25   cultured embryos.

26   **Study design, samples/materials, methods:** We used a standard wild type CD1 mouse model of

27   preimplanation embryo development and embryo culture to modulate atmospheric oxygen

28   tension and glucose media concentrations. Changes to p66Shc expression in mouse blastocysts

29   were measured using RT-qPCR, immunoblotting, and immunofluorescence with confocal

30   microscopy. Changes to oxidative phosphorylation metabolism were measured by total ATP

31   content and superoxide production. Statistical analyses were performed on a minimum of three

32   experimental replicates using Students' t-test or one-way ANOVA.

33   **Main results and the role of chance:** P66Shc is basally expressed during *in vivo* mouse

34   preimplantation development. Within *in vivo* blastocysts, p66Shc is primarily localized to the

35   cell periphery of the trophectoderm. Blastocysts cultured under atmospheric oxygen levels have

36   significantly increased p66Shc transcript and protein abundances compared to *in vivo* controls (p

37   < 0.05). However, phosphorylated serine 36 (S36) p66Shc to total p66Shc ratio decreased under

38   culture regardless of O_2 atmosphere used, supporting a shift in the mitochondrial fraction of

39   p66Shc. Total p66Shc localized to the cell periphery of the blastocyst trophectoderm and

40   phosphorylated S36 p66Shc displayed nuclear and cytoplasmic immunoreactivity, suggesting

41   distinct compartmentalization of phosphorylated S36 p66Shc and the remaining p66Shc fraction.

42   Glucose medium concentration did not significantly affect p66Shc expression or its localization.

43   Blastocysts cultured under low or high oxygen conditions exhibited significantly decreased

44   cellular ATP and increased superoxide production compared to *in vivo* derived embryos ($p <$

45   0.05).

46   **Limitations, reasons for caution:** This study associates embryonic p66Shc expression levels

47   with metabolic abnormalities but does not directly implicate p66Shc in metabolic changes.

48   **Wider implications of the findings:** This is the first study to show distinct immunolocalization

49   of p66Shc to the trophectoderm of blastocysts and that its levels are abnormally increased in

50   embryos exposed to culture conditions. Changes to p66Shc expression and/or localization could

51   serve as a molecular marker of embryo viability for clinical applications. The outcomes provide

52   insight into the potential metabolic role of p66Shc. Metabolic anomalies are induced even under

53   current best culture conditions, which could negatively impact trophectoderm and placental

54   development.

55   **Large scale data:** Not applicable.

56   **Study funding and competing interest(s):** Canadian Institutes of Health Research (CIHR)

57   operating funds, Ontario Graduate Scholarship. There are no competing interests.

58

59   **Key words:** blastocyst; embryo culture; metabolism; mitochondria; p66Shc; preimplantation

60   embryo; ROS, stress adaptor

61

62 **Introduction**

63   In assisted reproductive technologies (ARTs), embryo culture routinely follows *in vitro*

64 fertilization (IVF) to permit growth to the blastocyst stage. Despite improvements in culture

65 medium formulations and the use of physiological oxygen environments, the rate of successful

66 pregnancy after embryo culture remains considerably low. In 2014, the average live birth rate per

67 IVF cycle for women in Canada was 23% (CFAS, 2015). One possible reason for this low

68 success rate is the preimplantation embryo may be exposed to stress not normally encountered *in*

69 *vivo* as a result of adverse culturing conditions (Feuer and Rinaudo, 2012; Wale and Gardner,

70 2015). The mammalian preimplantation embryo may adapt to these adverse culture conditions,

71 however, these stress induced responses can result in major changes to gene expression,

72 epigenetic modifications, and cellular metabolism (Rinaudo and Schultz, 2004; Wale and

73 Gardner, 2012; de Waal *et al.*, 2014). These changes are currently undetectable by

74 morphological non-invasive assessment methods, and thus embryos selected by morphology for

75 transfer may still not be the most developmentally competent. This is a particular concern in

76 current efforts to reduce multiple pregnancies by single embryo transfer (Grady *et al.*, 2012).

77   To further advance embryo culture and optimize culture parameters, it is important to

78 understand the biological mechanisms of the preimplantation embryo and its interactions with

79 the maternal and *in vitro* environment. Metabolism has emerged as an important research avenue

80 in efforts to understand how culture conditions affect the developmental competence of early

81 embryos (Gardner *et al.*, 2001; Seli *et al.*, 2010; Wale and Gardner, 2013). Modulating oxygen

82 tension during embryo culture alters glucose metabolism, demonstrating that the culture

83 atmosphere can dramatically influence embryo metabolism and subsequent viability (Wale and

84 Gardner, 2012). This may affect the later stages of development in particular, as the

85   trophectoderm must generate ATP to power the Na$^+$/K$^+$ ATPases and form the blastocoele cavity

86   (Betts *et al.*, 1998; Houghton *et al.*, 2003). The adaptor protein p66Shc is responsive to oxygen

87   tension and is involved in the bovine embryo's oxidative stress response by promoting

88   permanent embryo arrest and apoptosis under adverse environmental conditions (Favetta *et al.*,

89   2007a; Betts *et al.*, 2014). P66Shc is a member of the Shc1 family of proteins with functions in

90   growth factor receptor signaling, reactive oxygen species (ROS) production, and oxidative

91   phosphorylation metabolism (Migliaccio *et al.*, 1997, 1999; Nemoto *et al.*, 2006; Acin-Perez *et*

92   *al.*, 2010). Loss-of-function studies in mouse embryonic fibroblasts (MEFs) and more recently in

93   HeLa cells provide evidence that p66Shc is involved in ATP production by oxidative

94   phosphorylation (Nemoto *et al.*, 2006; Soliman *et al.*, 2014). Dysregulated p66Shc function in

95   the mammalian embryo may therefore not only negatively impact development through high

96   ROS production inducing embryo arrest or apoptosis (Favetta *et al.*, 2004, 2007b; Betts *et al.*,

97   2014), but may also affect cellular metabolism (Favetta *et al.*, 2007a).

98   To define a new metabolic route in which preimplantation embryo culture may affect

99   early embryonic development, the objective of our study sought to determine if p66Shc

100 expression changes in cultured embryos compared to *in vivo* derived embryos, and if altered

101 p66Shc expression is a marker of altered embryo metabolism. In the following study, we use a

102 well-defined preimplantation mouse embryo culture model to modulate atmospheric conditions

103 (oxygen) and culture media (glucose concentration) to determine their effects on p66Shc

104 expression and readouts of oxidative phosphorylation metabolism. Our outcomes demonstrate

105 preimplantation developmental variations in p66Shc expression that are further exacerbated by

106 culture and correlate with aberrant mitochondrial ATP and ROS production.

Materials and Methods

Animal Source and Ethical Approval

Experimental protocols were approved by the Canadian Council of Animal Care and the

University of Western Ontario Animal Care and Veterinary Services (Watson #2010-021).

Female and male CD1 mice were obtained from Charles River Canada (St-Constant, Quebec,

Canada). Mice were conventionally housed with a 12h light/dark cycle and had access to food

and water *ad libitum*. For all experiments, mice were euthanized by CO_2 asphyxiation.

Embryo Collection and Culture

Three-to-four week old female mice were injected intraperitoneal with 7.5 IU pregnant

mare serum gonadotropin (Merck Animal Health, Canada) followed by injection of 7.5 IU

human chorionic gonadotropin (Merck Animal Health, Canada) 48 hours later. Female mice

were then placed with males for mating. Confirmation of mating was determined by checking for

the presence of a vaginal plug the next morning; presence of a vaginal plug indicated embryonic

day 0.5 (E0.5). Embryos were flushed with M2 medium (Sigma Aldrich, Canada) from the

oviducts and/or uteri of female mice according to the time post injection (hpi): zygotes (18 hpi),

2-cell embryos (44 hpi), 8-cell embryos (68 hpi) and blastocysts (90 hpi). Zygotes were briefly

incubated in M2 medium containing 1% hyaluronidase (Sigma Aldrich, Canada) to remove

cumulus cells. Embryos were washed twice in M2, then transferred to Extraction Buffer or

radioimmunoprecipitation assay buffer (RIPA buffer, 150 mM NaCl, 1% Triton X-100, 0.5%

sodium deoxycholate, 0.1% SDS, 50 mM Tris) until analysis, or to pre-equilibrated KSOMaa

Evolve medium supplemented with 1% bovine serum albumin (Zenith Biotech, USA). Embryos

were cultured under low (5% O_2) or high (in air) oxygen tensions in a 5% CO_2, 37°C incubator.

130   For glucose experiments, D- or L-glucose (Sigma Aldrich, Canada) was added to KSOMaa

131   Evolve to the desired concentration and embryos were cultured under low oxygen. For

132   transcriptional inhibition experiments, 10 mg/ml α-amanitin (Sigma Aldrich, Canada) in water

133   was diluted to 10 μg/ml in KSOMaa Evolve.

134

135   **Real time RT-qPCR**

136   Pools of twenty embryos collected from 1-3 mice were stored in Extraction Buffer (Life

137   Technologies, USA) at -80°C until use. Total RNA was extracted using the PicoPure RNA

138   isolation kit (Life Technologies, USA) according to the manufacturer's guidelines. For glucose

139   treatment experiments, 0.5 pg of exogenous luciferase mRNA (Promega, USA) was added to the

140   extract prior to ethanol precipitation. Eluted RNA was reverse transcribed to cDNA using

141   SuperScript III (Life Technologies, USA) according to manufacturer's instructions, with final

142   concentrations of 150 ng random hexamers (Life Technologies, USA) and 2 pmol p66Shc-

143   specific reverse primer (Table I). Real time qPCR was performed in a CFX384 thermocycler

144   (BioRad, Canada) with each reaction containing 7 μl PerfeCTa SYBR Green 2X SuperMix

145   (Quanta BioSciences, USA), 200 nM of forward and reverse primers (see Table I for all primer

146   sequences) and 4 μl cDNA (equivalent to 0.25 embryo per reaction). PCR conditions are as

147   follows: 95°C for 3 minutes, followed by 45 cycles of 95°C for 15 seconds, 59°C for 15 seconds,

148   and 72°C for 30 seconds. Relative transcript abundance was determined using the delta-delta CT

149   method using expression of *Ppia* and *H2afz*, or luciferase, for normalization (Mamo *et al.*, 2007).

150   To determine amplification specificity, PCR products after qPCR amplification of p66Shc in

151   blastocyst cDNA were purified using the PureLink Quick Gel Extraction and PCR Purification

152   Kit (Life Technologies, USA) according to manufacturer's instructions. PCR products were

153   sequenced by the Robarts Research Institute DNA Sequencing Facility (London, Ontario,

154   Canada). Amplified p66Shc PCR products displayed 96% sequence identity to *Mus musculus* src

155   homology 2 domain-containing transforming protein C1 (Shc1), transcript variant 1

156   (NM_001113331.2) after BLAST analysis (NCBI database), indicating specific amplification of

157   the p66Shc isoform.

158

159   **Western Blot Analysis**

160   Pools of 30-50 embryos collected from 2-4 mice were stored in RIPA buffer containing

161   protease and phosphatase inhibitor cocktails (Millipore, USA) at -80°C until use. Total protein

162   lysates were resolved on a 4-12% Bis-Tris gel (Life Technologies) and transferred to a PVDF

163   membrane (Millipore, USA). Membranes were blocked in 5% skim milk or 5% bovine serum

164   albumin in PBS with 0.1% Tween-20 (PBST, Sigma Aldrich) for 1 hour at room temperature,

165   followed by overnight incubation in primary antibody at the indicated concentration at 4°C.

166   Primary antibodies used: anti NT-Shc (Acris Antibodies, USA, 1:100), anti-(phospho S36)

167   p66Shc (Abcam, USA, 1:100), anti-(phospho Y239/Y240) p66Shc (Cell Signaling Technologies,

168   USA, 1:500), and HRP-conjugated anti β-actin (Sigma Aldrich, Canada, 1:20,000). Membranes

169   were then incubated in HRP-conjugated secondary antibody (Jackson Laboratories, USA).

170   Membranes were visualized by detection of Forte ECL (Millipore, USA). Densitometry analysis

171   was performed in Image Lab 4.0 (BioRad, USA).

172

173   **HT-22 culture and transfection**

174   The HT-22 cell line (immortalized mouse hippocampal cells) and human p66Shc-HA

175   expression plasmid were obtained from Dr. Robert Cumming (University of Western Ontario,

176   London, Canada). Cells were cultured in DMEM supplemented with 10% fetal bovine serum and

177   1% penicillin/streptomycin (Life Technologies, USA), at 37°C and 5% CO_2 in air. Cells were

178   transfected with the p66Shc-HA expression plasmid using Lipofectamine 3000 according to the

179   manufacturer's protocol (Life Technologies, USA), fixed in 4% paraformaldehyde in PBS and

180   processed for immunofluorescence and confocal microscopy.

181

182   **Immunofluorescence and Confocal Microscopy**

183   Embryos were fixed in 2% paraformaldehyde in PBS and permeabilized in 0.1% Triton

184   X-100 in PBS (Sigma Aldrich, Canada) for 30 minutes. Fixed cells were blocked in 5% normal

185   goat serum (Sigma Aldrich, Canada) for one hour at room temperature, followed by overnight

186   incubation in primary antibody at the indicated concentration at 4°C. Primary antibodies used:

187   anti NT-Shc (Acris Antibodies, 1:100), anti phospho-S36-p66Shc (Abcam, 1:100), anti CDX2

188   (Abcam, 1:100), anti HA-Alexa 647 (Santa Cruz, USA, 1:50). Embryos were incubated in rabbit-

189   anti-mouse Alexa 488 (Life Technologies) for 30 minutes, followed by incubation in goat-anti-

190   rabbit Alexa 488 (Life Technologies) for signal amplification. For CDX2 immunoreactivity,

191   embryos were incubated in goat-anti-rabbit Alexa 547 (Life Technologies). Cells were

192   counterstained with 0.5 µg/ml DAPI (Sigma Aldrich, Canada) and mounted on a glass

193   microscope slide in VectaShield antifade medium (Vector Laboratories, USA). Cells were

194   imaged with a laser scanning confocal microscope (Zeiss LSM510). Laser settings were

195   unchanged when detecting the same primary antibody.

196

197   **ATP content assay**

198   Pools of 5 blastocysts collected from individual mice after treatment under each oxygen

199   tension group were transferred to 96-well plates containing KSOMaa Evolve. ATP content was

200   measured using the Luminescent ATP Detection Assay Kit (Abcam, USA) according to

201   manufacturer's guidelines. Luminescence was quantified using an eight-point ATP standard

202   curve (0.78 pmol to 100 pmol) and normalized to blastocyst cell number.

203

204   **MitoSOX superoxide staining**

205   Blastocysts from each oxygen tension group were transferred to KSOMaa Evolve

206   containing 5 μM MitoSOX red mitochondrial superoxide indicator (Life Technologies, USA)

207   and incubated for 1 hour at 37°C, 5% CO_2, 5% O_2 (*in vivo* and low oxygen groups) or in air

208   (high oxygen groups). Blastocysts were transferred to a drop of PBS covered by embryo culture

209   grade mineral oil (Zenith Biotech, USA) for imaging. Blastocysts were imaged using laser

210   scanning confocal microscopy (Zeiss LSM510). Relative fluorescence was quantified by

211   measuring the mean gray value in Image J (NIH). Only blastocyst images with visible inner cell

212   mass were quantified for fluorescence and compared between groups.

213

214   **Blastocyst Cell Counts**

215   Blastocysts were fixed in 4% paraformaldehyde in PBS, permeabilized in 0.2% Triton X-

216   100 in PBS, and stained with DAPI for 1 hour at room temperature. Stained blastocysts were

217   imaged using laser scanning confocal microscopy, with three z-stacks taken per embryo. DAPI-

218   positive nuclei from three stacks were counted using ImageJ.

219

220   **Statistical Analyses**

221   Experiments were performed a minimum of three times using independent replicates with

222   the indicated sample sizes. Statistical analyses were performed in Graph Pad Prism (6.0) for

223   Student's t-test (unpaired, two-tailed, equal variance) or one-way analysis of variance (ANOVA)

224   followed by Tukey's honestly significant difference (HSD) test to correct for multiple

225   comparisons. Values presented in figures are the mean ± the standard error of the mean (SEM).

226   Probability values less than 0.05 ($p < 0.05$) were considered statistically significant.

227

228   **Results**

229   **P66Shc expression increases in blastocysts during mouse preimplantation development**

230   P66Shc expression has been previously detected in bovine (Favetta *et al.*, 2004) and

231   murine embryos (Ren *et al.*, 2014), but an analysis of expression during the progression of

232   mouse preimplantation development *in vivo* has not been carried out. To determine the

233   expression profile of p66Shc during preimplantation development, we performed real time RT-

234   qPCR and immunoblotting on pools of embryos from four developmental stages. P66Shc

235   transcript and protein were detectable in all stages observed. We observed a significant increase

236   in both transcript and protein abundance from the 8-cell to blastocyst stages (Figure 1A, B). To

237   determine the cellular localization of p66Shc during preimplantation development, we performed

238   whole mount immunofluorescence followed by confocal microscopy using a p66Shc-specific

239   antibody on embryos from six developmental stages. We observed p66Shc immunoreactivity

240   throughout the cytoplasm of pre-compaction stage embryos (Figure 2A-D), with restriction to the

241   apical cell periphery of compacted 16 cell morulae (Figure 2E). To determine if p66Shc

242   localization is restricted to the trophectoderm lineage, we co-stained blastocysts with CDX2. Of

243   all blastocysts observed, p66Shc showed detectable cell periphery localization in only CDX2

244   positive cells. P66Shc immunoreactivity was undetectable in CDX2 negative cells (Figure 2F).

245   These results indicate that p66Shc expression is normally upregulated in the blastocyst and may

246   be restricted primarily to the trophectoderm of *in vivo* produced blastocysts.

247

248   **Validation of NT-Shc antibody specificity**

249   To verify that the antibodies used to detect p66Shc and phosphorylated (S36) p66Shc

250   only recognized the 66-kDa Shc isoform by immunofluorescence confocal microscopy, we

13

251   cultured mature neurons known to have undetectable basal p66Shc expression (Ventura *et al.*,

252   2002). We performed immunofluorescence using both antibodies on the mouse HT-22

253   hippocampal cell line. HT-22 cells transfected with a HA-tagged p66Shc DNA construct showed

254   p66Shc and HA immunoreactivity, while non-transfected cells showed no detectable p66Shc or

255   HA immunoreactivity (Supplemental Figure 1A). Transfected HT-22 cells also displayed

256   phosphorylated S36 p66Shc and HA immunoreactivity compared to undetectable levels in non-

257   transfected cells (Supplemental Figure 1B). These results validate the use of these antibodies for

258   immunofluorescent detection of p66Shc and S36-phosphorylated p66Shc cell localization in

259   mouse preimplantation embryos.

260

261   **P66Shc expression is sensitive to oxygen tension, but not glucose concentration, during**

262   **embryo culture**

263   Under *in vivo* conditions, p66Shc expression levels may be fine-tuned to prevent adverse

264   developmental events. Given our observations within *in vivo* derived mouse embryos, we then

265   aimed to determine whether certain embryo culture conditions induce aberrant changes in

266   embryonic p66Shc expression levels. Mouse zygotes were cultured to three developmental stages

267   under low oxygen tension (5% O_2) or high oxygen tension (21% O_2). Real time RT-qPCR was

268   performed on pools of embryos to determine changes in p66Shc transcript abundance.

269   Blastocysts examined after 96 hours of culture showed increasing p66Shc transcript abundance

270   with increasing oxygen tension (Figure 3A). This increase was dependent on *de novo*

271   transcription of p66Shc, as the increase in p66Shc abundance was abolished in blastocysts

272   cultured at high oxygen tension in the presence of the transcriptional inhibitor α-amanitin

273   (Figure 3B). It is interesting to note that some p66Shc transcripts were still detectable in treated

274   blastocysts, suggesting that maternally stored p66Shc may still be present at the blastocyst stage

275   (Figure 3B). Overall, these observations suggest that p66Shc is actively transcribed by the

276   embryo under atmospheric oxygen conditions.

277   We next aimed to determine if p66Shc protein abundance also increased under culture

278   and high oxygen. Immunoblotting for total p66Shc on pools of embryos showed a significant

279   increase in p66Shc protein abundance in cultured blastocysts (Figure 4A). This induction of

280   p66Shc expression was unique to the blastocyst stage, as p66Shc transcript abundance decreased

281   and protein abundance was unchanged in cultured 2-cell and 8-cell embryos (Supplemental

282   Figure 2A and B). We then saw that increasing oxygen tension significantly decreased the

283   phosphorylated S36 p66Shc to total p66Shc ratio in blastocysts, suggesting a possible change in

284   the mitochondrial fraction of p66Shc in cultured blastocysts (Figure 4B). Oxygen tension did not

285   alter the phosphorylated Y239/Y240 p66Shc to total p66Shc ratio (Figure 4C). These are two

286   residues on Shc1 proteins that are known to be phosphorylated after interaction with receptor

287   tyrosine kinases (Gotoh *et al.*, 1997). This result suggests that the shift in the 66-kDa band seen

288   in cultured blastocysts may be due to an alternative (e.g. Ser138, Y317) or novel post-

289   translational modification induced by culture.

290   To determine if p66Shc cellular localization changed with embryo culture, cultured

291   blastocysts were stained for p66Shc immunoreactivity and were compared to freshly flushed, *in*

292   *vivo* derived blastocysts. Blastocysts cultured in high oxygen conditions showed an increase in

293   p66Shc fluorescence intensity and detectable diffuse p66Shc staining in putative ICM cells,

294   compared to *in vivo* and low oxygen cultured blastocysts (Figure 5A-C). To determine the

295   localization of phosphorylated S36 p66Shc, cultured blastocysts were stained for phosphorylated

296   S36 p66Shc immunoreactivity and compared to *in vivo* controls. Consistent with the

297   immunoblotting results, neither the fluorescence levels of phosphorylated S36 p66Shc nor its

298   localization appeared to change between treatment groups. However, phosphorylated S36

299   p66Shc did show a distinct cellular localization pattern compared to total p66Shc, showing

300   cytoplasmic and nuclear immunoreactivity in the outer and inner cells of the blastocyst (Figure

301   6A-C). In addition, phosphorylated S36 p66Shc was also detectable in inner cells of the *in vivo*

302   produced blastocyst while total p66Shc was not, indicating that there may be differences in

303   sensitivity between the two p66Shc antibodies (Figures 5A and 6A). The localization pattern

304   suggests that the phosphorylated S36 p66Shc fraction in blastocysts produced *in vivo* or in

305   culture may be localized to a distinct compartment in the cytoplasm or nucleus compared to non-

306   phosphorylated, or p66Shc phosphorylated at a different residue.

307   In addition to its role in mediating the oxidative stress response, several studies have

308   implicated p66Shc in regulating cellular glucose uptake through growth factor receptor signaling,

309   actin cytoskeleton regulation, or modulation of anaerobic respiration (Natalicchio *et al.*, 2009;

310   Soliman *et al.*, 2014). Thus, we next aimed to determine if p66Shc expression is sensitive to

311   medium glucose concentration, another component modified in embryo culture to simulate *in*

312   *vivo* microenvironmental conditions. We cultured 8-cell stage embryos for 24 hours in KSOM

313   varying in glucose concentrations under low oxygen tension: 0.2 mM (standard KSOM), 3.4 mM

314   (equivalent to normal mouse oviductal glucose levels, (Gardner and Leese, 1990)), 30 mM D-

315   glucose (hyperglycemia, (Moley *et al.*, 1998)) and 30 mM L-glucose to control for increased

316   osmolarity. We observed that embryos cultured in 30 mM D-glucose have decreased rates of

317   blastocyst cavitation (Figure 7A). The embryos did not fail to cavitate due to glucose toxicity, as

318   18 hours culture in 0.2 mM D-glucose rescued cavitation (Figure 7B). Furthermore, cell number

319   in non-cavitated embryos did not significantly change with high glucose culture compared to

320   control, suggesting that these embryos were not developing slower than the controls (Figure 7C).

321   To determine if p66Shc expression changed during culture in high glucose, we performed

322   RT-qPCR and immunoblotting for p66Shc in pools of blastocysts cultured in the four glucose

323   concentrations. Neither transcript levels nor protein abundance significantly changed in embryos

324   cultured in varying glucose conditions (Figure 8A-B), suggesting that p66Shc expression levels

325   are not sensitive to increased glucose in embryo culture media. To determine if p66Shc cellular

326   localization changed with glucose concentration, embryos cultured in 30 mM D-glucose were

327   stained for p66Shc immunoreactivity and compared to embryos cultured in KSOM. We saw

328   comparable peripheral and cytoplasmic p66Shc immunoreactivity in non-cavitated embryos after

329   high glucose culture compared to controls, suggesting that p66Shc cellular localization is not

330   impacted by media glucose concentrations (Figure 8C).

331

332   **Changes to p66Shc expression in culture correlate with altered embryo metabolism**

333   To determine if increased p66Shc expression levels in cultured embryos could be a

334   marker of altered embryo metabolism, we performed two metabolic assays on blastocysts

335   derived *in vivo* and after culture under low and high oxygen. We first assessed total ATP content

336   of blastocysts from each group, and observed that ATP levels per cell significantly decreased in

337   blastocysts cultured under low oxygen compared to *in vivo* blastocysts (Figure 9A). As oxidative

338   phosphorylation in the trophectoderm is the major source of cellular ATP in the blastocyst

339   (Houghton, 2006), we then assayed for production of superoxide in the same treatment groups.

340   Superoxide is a free radical produced as a by-product of oxidative phosphorylation that is

341   normally present at low levels and is readily scavenged by superoxide dismutase. Blastocysts

342   were incubated in MitoSOX red superoxide indicator and imaged using confocal microscopy.

343   We observed that blastocysts cultured under low and high oxygen showed significantly higher

344   MitoSOX fluorescence compared to *in vivo* controls, suggesting increased superoxide production

345   or decreased antioxidant scavenging in these culture conditions (Figure 9B). Our results suggest

346   that even under low oxygen conditions, cultured blastocysts contain less ATP and increased

347   superoxide levels, correlating with increased mRNA and protein abundance of p66Shc.

348

Discussion

349

350   Here we demonstrate that p66Shc is basally expressed in mouse preimplantation embryos

351 and its expression is altered by embryo culture. We also show that dysregulated p66Shc

352 expression coincides with metabolic changes in culture that may negatively affect embryo

353 developmental viability. Our results suggest that p66Shc is an oogenetic-stored transcript that is

354 degraded during the maternal-to-embryonic transition, later upregulated by the blastocyst stage,

355 and predominately located at the cell periphery of trophectoderm cells. Blastocysts grown *in*

356 *vitro* show increasing p66Shc expression with increasing oxygen tension, coupled with

357 alterations to phosphorylated residues that have implications in the protein's cellular

358 compartmentalization and function. These changes appear to be oxygen-sensitive, while

359 changing media glucose concentrations did not significantly affect p66Shc expression levels in

360 the blastocyst. Lastly, we are the first to correlate these changes in culture and high oxygen

361 tension to dysregulated ATP and superoxide production within *in vitro* produced blastocysts.

362   Our expression analysis of p66Shc during *in vivo* blastocyst development suggests that

363 p66Shc is normally upregulated during the eight-cell embryo to blastocyst transition. This basal

364 level of expression during *in vivo* development implies that despite promoting apoptosis, p66Shc

365 expression maybe necessary for survival and prevent blastocysts from being selected against

366 during development. One possible biological function of p66Shc during preimplantation

367 development may be the promotion of oxidative phosphorylation. Basal oxygen consumption in

368 66Shc-null MEFs decreases by 30-50% with no change in mitochondrial or cytochrome c

369 content, with a compensatory increase in ATP production by anaerobic respiration (Nemoto *et*

370 *al.*, 2006). There is also evidence suggesting that in MEFs, p66Shc forms a complex with

371 cytochrome c in the inner mitochondrial membrane to regulate pyruvate dehydrogenase kinase

372   (PDK), ultimately regulating the activity of pyruvate dehydrogenase (PDH) depending on the

373   redox state of cytochrome c (Acin-Perez *et al.*, 2010). In the mouse blastocyst, the trophectoderm

374   produces ATP through oxidative phosphorylation to support development, but the ICM is

375   relatively metabolically quiescent (Houghton, 2006). Metabolic differences between the two

376   embryonic linages could account for our immunolocalization results, as p66Shc appears to

377   localize predominately to the trophectoderm *in vivo* and under low oxygen conditions,

378   suggesting that p66Shc could be involved in trophectoderm metabolism. Although our study did

379   not directly test the role of p66Shc in oxidative phosphorylation, we have correlated increasing

380   p66Shc transcript and protein abundances after embryo culture with alterations to ATP and

381   superoxide production, suggesting that dysregulated p66Shc levels in the embryo may have a

382   negative impact on embryo metabolism.

383   Studies of p66Shc in mammalian embryos have thus far focused primarily on the

384   apoptosis- and senescence-promoting functions of p66Shc, basally or in stress-inducing culture

385   conditions. In bovine preimplantation embryos, siRNA-mediated knockdown of p66Shc reduces

386   levels of intracellular ROS, DNA damage, and apoptosis in untreated and oxidant-treated culture

387   conditions (Betts *et al.*, 2014). Bovine preimplantation embryos exhibit high levels of

388   developmental arrest (>50%) in culture (Leidenfrost *et al.*, 2011), likely due to suboptimal

389   culture conditions, which could result in increased p66Shc transcript levels, leading to

390   senescence (permanent embryo arrest) and apoptosis. Due to species-specific differences in early

391   development, or better optimized conditions, mouse preimplantation embryos from inbred strains

392   exhibit high developmental rates with >75% of zygotes reaching the blastocyst stage in

393   optimized media and low oxygen conditions (Karagenc *et al.*, 2004). It is possible that p66Shc

394   expression is carefully regulated during preimplantation development, such that both abnormally

395   high and low p66Shc expression levels are detrimental to the embryo.

396   Consistent with our findings in our mouse embryo culture model, there is strong evidence

397   associating p66Shc induction under adverse embryo culture conditions. Bovine embryos under

398   oviductal epithelial cell co-culture growth conditions show significantly increased p66Shc

399   transcript abundance compared to culture under chemically defined synthetic oviductal fluid

400   media at lower oxygen tension. This increase was associated with increased markers of oxidative

401   stress (intracellular ROS, DNA damage) and embryo arrest (Favetta *et al.*, 2007b). Mouse

402   embryos treated with arsenic show increasing p66Shc immunofluorescence intensity, suggesting

403   that p66Shc may mediate a stress response to arsenic (Zhang *et al.*, 2010). Preimplantation

404   development under both cases improved when p66Shc was knocked down by RNA interference

405   (Favetta *et al.*, 2007a; Betts *et al.*, 2014; Ren *et al.*, 2014). Previous RNA-interference

406   experiments may have normalized an adverse environment-induced "spike" in p66Shc

407   expression, but not completely deplete the embryo of maternal- or zygotic-derived p66Shc, thus

408   masking any loss-of-function phenotype. Maternally-derived p66Shc function may be important

409   to preimplantation development, as embryo cleavage and blastocyst development is impaired

410   when p66Shc is knocked down in immature bovine oocytes (Favetta *et al.*, 2007a). We are the

411   first to show that p66Shc transcript and protein expression is upregulated at the blastocyst stage

412   during mouse *in vivo* development, indicating that p66Shc may also have an important

413   physiological function other than promoting apoptosis and embryo arrest.

414   The induction of p66Shc transcription in cultured blastocysts appears to be specific to

415   oxygen, as increasing media glucose concentrations did not significantly change p66Shc

416   transcript abundance compared to controls. Oxygen-sensitive induction in our results is

417   consistent with findings that p66Shc transcription can be regulated by the Nrf2-antioxidant

418   response element (ARE) pathway under stress-inducing conditions. Chromatin

419   immunoprecipitation assays performed in hemin-treated human erythroleukemic cells

420   demonstrated that Nrf2 binds to an ARE enhancer upstream of the transcriptional start site of

421   p66Shc and that Nrf2 induction of expression is isoform-specific (Miyazawa and Tsuji, 2014).

422   This could be the upstream mechanism in our model of p66Shc transcriptional upregulation in

423   blastocysts cultured under high oxygen. High media glucose concentrations did not significantly

424   change p66Shc expression in blastocysts, but did affect cavitation. This is consistent with

425   previous reports of hyperglycemic conditions negatively affecting blastocyst development

426   (Fraser *et al.*, 2007). Thus it is unlikely that the cell's response to high glucose regulates the

427   transcription of p66Shc, but instead may affect other genes known to be involved in cavitation

428   (e.g. *Atp1b1, Aqp3, Aqp9, Cdh1*). Furthermore, it is not known whether p66Shc is important for

429   the regulation of glucose uptake in preimplantation embryos or if this function is dependent on

430   mTOR or growth factor receptor signaling pathways (Natalicchio *et al.*, 2009; Soliman *et al.*,

431   2014). It is possible that p66Shc could mediate a response to high glucose levels in embryos

432   independent of an increase in its transcript or protein abundance, through phosphorylation of

433   certain residues.

434   It is possible that culture conditions increase p66Shc expression to promote its apoptotic

435   functions, removing it from its metabolic function in the mitochondria. Our results suggest that

436   culture-mediated changes to phosphorylated residues on p66Shc may impact its cellular

437   compartmentalization and may ultimately be a key factor in its cellular function. Subcellular

438   fractionation of untreated MEF lysates showed that p66Shc is detectable in the soluble,

439   mitochondrial, and endoplasmic reticulum fractions (Orsini *et al.*, 2004). Phosphorylation of the

440   serine-36 residue, which is unique to the 66 kDa isoform of the Shc1 family, has been implicated

441   in its cellular localization. Serine-36 phosphorylation of p66Shc under oxidizing conditions

442   increases its association with the prolyl isomerase Pin-1, ultimately resulting in p66Shc

443   translocation to the mitochondria. Fibroblasts lacking Pin-1 have a decreased mitochondrial

444   fraction of p66Shc after H_2O_2 treatment compared to wild type fibroblasts, linking the

445   modification of this residue to the protein's mitochondrial localization (Pinton *et al.*, 2007). In

446   our study, blastocysts cultured under low or high oxygen conditions show decreased

447   phosphorylated 36 to total p66Shc ratios, suggesting that these conditions may decrease the

448   mitochondrial fraction of p66Shc despite an increase in total p66Shc protein abundance. This

449   alteration in cellular localization may affect p66Shc's functions in the mitochondria, which our

450   results of altered embryo metabolism may reflect.

451   Despite using optimal culture conditions, both p66Shc expression and the metabolic

452   parameters measured were significantly altered in blastocysts grown under low oxygen tension.

453   No significant difference between increased superoxide production in blastocysts after culture in

454   low or high oxygen tension suggests that oxidative phosphorylation metabolism may be

455   adversely affected regardless of oxygen tension, or that there is another parameter in the

456   microenvironment that must be further optimized to limit metabolic alterations in cultured

457   embryos. Levels of p66Shc may therefore be an indicator of altered blastocyst metabolism,

458   particularly of the trophectoderm, which is responsible for generating nearly all of the

459   blastocyst's ATP content (Houghton, 2006). Altered expression levels and/or p66Shc function in

460   culture may lead to adverse trophectoderm development through increases in ROS-mediated

461   apoptosis or decreases in ATP production, which may impact implantation and placentation. Our

462   study did not follow up on peri- and post-implantation stage embryos and p66Shc expression

463　levels, but we suspect that p66Shc expression is likely altered in the trophoblast or post-

464　implantation trophoblast-derived tissues after embryo culture. Supporting this is evidence that

465　p66Shc CpG promoter methylation is decreased in human placental tissue of intrauterine growth

466　restricted neonates compared to neonates appropriate and small for gestational age (Tzschoppe *et*

467　*al.*, 2013). This is also consistent with the finding most culture-induced embryo abnormalities

468　affect the trophoblast and placenta, and to a lesser extent the fetal tissues (Fauque *et al.*, 2010; de

469　Waal *et al.*, 2014). For clinical applications, using increased p66Shc expression as a molecular

470　marker of altered metabolism may impact which blastocyst may be the most developmentally

471　competent for embryo transfer.

472

473　**Acknowledgements**

478

479　**Authors' Roles**

480　Study conception and design: NAE, AJW, DHB. Performed the experiments: NAE. Data

481　analysis: NAE, AJW, DHB. Drafted and proofread the manuscript: NAE, AJW, DHB.

482

483　**Funding**

486

487   **Conflict of Interest**

488   None to declare.

489

490   **References**

491   Acin-Perez R, Hoyos B, Gong J, Vinogradov V, Fischman DA, Leitges M, Borhan B, Starkov A,

492   Manfredi G, Hammerling U. Regulation of intermediary metabolism by the PKCdelta

493   signalosome in mitochondria. *FASEB J* 2010;**24**:5033–5042.

494   Betts DH, Bain NT, Madan P. The p66(Shc) adaptor protein controls oxidative stress response in

495   early bovine embryos. *PLoS One* 2014;**9**:e86978.

496   Betts DH, Barcroft LC, Watson AJ. Na/K-ATPase-mediated 86Rb+ uptake and asymmetrical

497   trophectoderm localization of alpha1 and alpha3 Na/K-ATPase isoforms during bovine

498   preattachment development. *Dev Biol* 1998;**197**:77–92.

499   CFAS. Human Assisted Reproduction 2015 Live Birth Rates for Canada. 2015;Available from:

500   http://www.cfas.ca/index.php?option=com_content&view=article&id=1415%3Ahuman-

501   assisted-reproduction-2015-live-birth-rates-for-canada&catid=929%3Apress-

502   releases&Itemid=130.

503   Fauque P, Mondon F, Letourneur F, Ripoche M-A, Journot L, Barbaux S, Dandolo L, Patrat C,

504   Wolf J-P, Jouannet P, *et al.* In vitro fertilization and embryo culture strongly impact the

505   placental transcriptome in the mouse model. *PLoS One* 2010;**5**:e9218.

506   Favetta LA, Madan P, Mastromonaco GF, St John EJ, King WA, Betts DH. The oxidative stress

507   adaptor p66Shc is required for permanent embryo arrest in vitro. *BMC Dev Biol*

508   2007a;**7**:132.

509   Favetta LA, Robert C, St John EJ, Betts DH, King WA. p66shc, but not p53, is involved in early

510   arrest of in vitro-produced bovine embryos. *Mol Hum Reprod* 2004;**10**:383–392.

511   Favetta LA, St John EJ, King WA, Betts DH. High levels of p66shc and intracellular ROS in

512   permanently arrested early embryos. *Free Radic Biol Med* 2007b;**42**:1201–1210.

513   Feuer S, Rinaudo P. Preimplantation stress and development. *Birth Defects Res C Embryo Today*

514   2012;**96**:299–314.

515   Fraser RB, Waite SL, Wood KA, Martin KL. Impact of hyperglycemia on early embryo

516   development and embryopathy: in vitro experiments using a mouse model. *Hum Reprod*

517   2007;**22**:3059–3068.

518   Gardner DK, Lane M, Stevens J, Schoolcraft WB. Noninvasive assessment of human embryo

519   nutrient consumption as a measure of developmental potential. *Fertil Steril* 2001;**76**:1175–

520   1180.

521   Gardner DK, Leese HJ. Concentrations of nutrients in mouse oviduct fluid and their effects on

522   embryo development and metabolism in vitro. *J Reprod Fertil* 1990;**88**:361–368.

523   Gotoh N, Toyoda M, Shibuya M. Tyrosine phosphorylation sites at amino acids 239 and 240 of

524   Shc are involved in epidermal growth factor-induced mitogenic signaling that is distinct

525   from Ras/mitogen-activated protein kinase activation. *Mol Cell Biol* 1997;**17**:1824–1831.

526   Grady R, Alavi N, Vale R, Khandwala M, McDonald SD. Elective single embryo transfer and

527   perinatal outcomes: A systematic review and meta-analysis. *Fertil Steril* 2012;**97**:324–331.

528   Elsevier Inc.

529   Houghton FD, Humpherson PG, Hawkhead J a, Hall CJ, Leese HJ. Na+, K+, ATPase activity in

530   the human and bovine preimplantation embryo. *Dev Biol* 2003;**263**:360–366.

531   Houghton FD. Energy metabolism of the inner cell mass and trophectoderm of the mouse

532   blastocyst. *Differentiation* 2006;**74**:11–18.

533   Karagenc L, Sertkaya Z, Ciray N, Ulug U, Bahçeci M. Impact of oxygen concentration on

534   embryonic development of mouse zygotes. *Reprod Biomed Online* 2004;**9**:409–417.

535   Reproductive Healthcare Ltd, Duck End Farm, Dry Drayton, Cambridge CB23 8DB, UK.

536   Leidenfrost S, Boelhauve M, Reichenbach M, Güngör T, Reichenbach HD, Sinowatz F, Wolf E,

537   Habermann FA. Cell arrest and cell death in mammalian preimplantation development:

538   Lessons from the bovine model. *PLoS One* 2011;**6.**:

539   Mamo S, Gal AB, Bodo S, Dinnyes A. Quantitative evaluation and selection of reference genes

540   in mouse oocytes and embryos cultured in vivo and in vitro. *BMC Dev Biol* 2007;**7**:14.

541   Migliaccio E, Giorgio M, Mele S, Pelicci G, Reboldi P, Pandolfi PP, Lanfrancone L, Pelicci PG.

542   The p66shc adaptor protein controls oxidative stress response and life span in mammals.

543   *Nature* 1999;**402**:309–313.

544   Migliaccio E, Mele S, Salcini AE, Pelicci G, Lai KM, Superti-Furga G, Pawson T, Fiore PP Di,

545   Lanfrancone L, Pelicci PG. Opposite effects of the p52shc/p46shc and p66shc splicing

546   isoforms on the EGF receptor-MAP kinase-fos signalling pathway. *EMBO J* 1997;**16**:706–

547   716.

548   Miyazawa M, Tsuji Y. Evidence for a novel antioxidant function and isoform-specific regulation

549   of the human p66Shc gene. *Mol Biol Cell* 2014;**25**:2116–2127.

550   Moley KH, Chi MM, Knudson CM, Korsmeyer SJ, Mueckler MM. Hyperglycemia induces

551   apoptosis in pre-implantation embryos through cell death effector pathways. *Nat Med*

552   1998;**4**:1421–1424.

553   Natalicchio A, Stefano F De, Perrini S, Laviola L, Cignarelli A, Caccioppoli C, Quagliara A,

554   Melchiorre M, Leonardini A, Conserva A, *et al.* Involvement of the p66Shc protein in

555   glucose transport regulation in skeletal muscle myoblasts. *Am J Physiol Endocrinol Metab*

556   2009;**296**:E228–E237.

557   Nemoto S, Combs CA, French S, Ahn BH, Fergusson MM, Balaban RS, Finkel T. The

558   mammalian longevity-associated gene product p66shc regulates mitochondrial metabolism.

559   *J Biol Chem* 2006;**281**:10555–10560.

560   Orsini F, Migliaccio E, Moroni M, Contursi C, Raker VA, Piccini D, Martin-Padura I, Pelliccia

561   G, Trinei M, Bono M, *et al.* The life span determinant p66Shc localizes to mitochondria

562   where it associates with mitochondrial heat shock protein 70 and regulates trans-membrane

563   potential. *J Biol Chem* 2004;**279**:25689–25695.

564   Pinton P, Rimessi A, Marchi S, Orsini F, Migliaccio E, Giorgio M, Contursi C, Minucci S,

565   Mantovani F, Wieckowski MR, *et al.* Protein kinase C beta and prolyl isomerase 1 regulate

566   mitochondrial effects of the life-span determinant p66Shc. *Science* 2007;**315**:659–663.

567   Ren K, Li X, Yan J, Huang G, Zhou S, Yang B, Ma X, Lu C. Knockdown of p66Shc by siRNA

568   injection rescues arsenite-induced developmental retardation in mouse preimplantation

569   embryos. *Reprod Toxicol* 2014;**43**:8–18.

570   Rinaudo P, Schultz RM. Effects of embryo culture on global pattern of gene expression in

571   preimplantation mouse embryos. *Reproduction* 2004;**128**:301–311.

572   Seli E, Vergouw CG, Morita H, Botros L, Roos P, Lambalk CB, Yamashita N, Kato O, Sakkas

573   D. Noninvasive metabolomic profiling as an adjunct to morphology for noninvasive embryo

574   assessment in women undergoing single embryo transfer. *Fertil Steril* 2010;**94**:535–542.

575   Elsevier Ltd.

576   Soliman MA, Abdel Rahman AM, Lamming DW, Birsoy K, Pawling J, Frigolet ME, Lu H,

577   Fantus IG, Pasculescu A, Zheng Y, *et al.* The adaptor protein p66Shc inhibits mTOR-

578   dependent anabolic metabolism. *Sci Signal* 2014;**7**:ra17.

579   Tzschoppe A, Doerr H, Rascher W, Goecke T, Beckmann M, Schild R, Struwe E, Geisel J, Jung

580   H, Dötsch J. DNA methylation of the p66Shc promoter is decreased in placental tissue from

581   women delivering intrauterine growth restricted neonates. *Prenat Diagn* 2013;**33**:484–491.

582   Ventura A, Luzi L, Pacini S, Baldari CT, Pelicci PG. The p66Shc longevity gene is silenced

583   through epigenetic modifications of an alternative promoter. *J Biol Chem* 2002;**277**:22370–

584   22376.

585   Waal E de, Mak W, Calhoun S, Stein P, Ord T, Krapp C, Coutifaris C, Schultz RM, Bartolomei

586   MS. In vitro culture increases the frequency of stochastic epigenetic errors at imprinted

587   genes in placental tissues from mouse concepti produced through assisted reproductive

588   technologies. *Biol Reprod* 2014;**90**:22.

589   Wale PL, Gardner DK. Oxygen Regulates Amino Acid Turnover and Carbohydrate Uptake

590   During the Preimplantation Period of Mouse Embryo Development. *Biol Reprod*

591   2012;**87**:24–24.

592   Wale PL, Gardner DK. Oxygen affects the ability of mouse blastocysts to regulate ammonium.

593   *Biol Reprod* 2013;**89**:75.

594   Wale PL, Gardner DK. The effects of chemical and physical factors on mammalian embryo

595   culture and their importance for the practice of assisted human reproduction. *Hum Reprod*

596   *Update* 2015;**22**:dmv034 – .

597   Zhang C, Liu C, Li D, Yao N, Yuan X, Yu A, Lu C, Ma X. Intracellular redox imbalance and

598   extracellular amino acid metabolic abnormality contribute to arsenic-induced developmental

30

599   retardation in mouse preimplantation embryos. *J Cell Physiol* 2010;**222**:444–455.

600

601

602   **Figure Legends**

603   **Figure 1**. p66Shc expression increases during mouse preimplantation development *in vivo*. (A)

604   RT-qPCR for p66Shc relative transcript abundance was performed on three replicates of pools of

605   20 embryos per stage. P66Shc relative transcript abundance significantly increases from eight

606   cell to blastocyst-stage embryos (n=3, mean ± SEM, p=0.0476 1W-ANOVA). (B)

607   Immunoblotting for total p66Shc protein abundance was performed on three replicates of pools

608   of 30-50 embryos per stage. P66Shc relative protein abundance increases from eight cell to

609   blastocyst-stage embryos (n=3, mean ± SEM, p=0.0331 1W-ANOVA). A representative blot is

610   shown.

611

612   **Figure 2**. p66Shc progressively localizes to the cell periphery during mouse preimplantation

613   development. Immunofluorescence and confocal microscopy for p66Shc was performed on 10-

614   20 embryos per stage. Representative confocal images are shown: (A) Zygote (B) 2-cell embryo

615   (C) 4-cell embryo (D) 8-cell non-compacted embryo (E) 8-16 cell compacted morula (F)

616   Blastocyst, counterstained for CDX2 (G) Primary antibody omitted. Green = p66Shc, Red =

617   CDX2, Blue = DAPI. Scale bar = 20 μm.

618

619   **Figure 3**. Culture and high oxygen tension increases the relative p66Shc mRNA abundance in

620   blastocysts. (A) RT-qPCR for p66Shc was performed on four replicates of pools of 20

621   blastocysts. There is a significant increase in p66Shc mRNA abundance in blastocysts cultured at

622   high oxygen tension compared to in vivo controls (n=4, mean ± SEM, p=0.0305 1W-ANOVA).

623   (B) Blastocysts cultured for 24h in 10 μg/ml α-amanitin showed significantly decreased p66Shc

624   transcript abundance compared to controls (n=3, mean ± SEM, p=0.0477 Student's t-test).

625

626 **Figure 4.** Culture and high oxygen tension increases the relative p66Shc protein abundance in

627 blastocysts. (A) Immunoblotting for p66Shc was performed on four replicates of pools of 50

628 blastocysts. P66Shc protein abundance significantly increases in blastocysts cultured at low

629 oxygen tension compared to in vivo controls (n=4, mean ± SEM, p=0.0306 1W-ANOVA). A

630 representative blot is shown. (B) Immunoblotting for phosphorylated p66Shc on serine 36 (S36)

631 and total p66Shc was performed on three replicates of pools of 40-50 blastocysts. The ratio of

632 phospho (S36)-p66Shc:total p66Shc significantly decreases in cultured blastocysts compared to

633 controls (n=3, mean ± SEM, p=0.0057 for low O_2; p=0.0219 for high O_2 1W-ANOVA). A

634 representative blot is shown. (C) Immunoblotting for phosphorylated Y239/Y240-p66Shc and

635 total p66Shc was performed on three replicates of pools of 20-30 blastocysts. The ratio of

636 phosphor Y239/Y240-p66Shc:total p66Shc does not significantly in cultured blastocysts

637 compared to controls (n=3, mean ± SEM, p=0.5043, 1W-ANOVA). A representative blot is

638 shown.

639

640 **Figure 5**. Total p66Shc becomes detectable in the inner cells of blastocysts cultured under

641 atmospheric oxygen tension. Representative immunofluorescence and confocal microscopy

642 images for total p66Shc in pools of 10-15 blastocysts per treatment group. (A) *In vivo* flushed

643 blastocysts. (B) Blastocysts after 96 h culture under low oxygen tension. (C) Blastocysts after 96

644 h culture under high oxygen tension. Green = p66Shc, Blue = DAPI. Scale bar = 20 μm.

645

646 **Figure 6**. Phosphorylated S36 p66Shc localization does not change in cultured blastocysts.

647 Representative immunofluorescence and confocal microscopy images for phosporylated (S36)

648   p66Shc in pools of 15-20 blastocysts per treatment group. (A) *In vivo* flushed blastocysts. (B)

649   Blastocysts after 96 h culture under low oxygen tension. (C) Blastocysts after 96 h culture under

650   high oxygen tension. Green = p66Shc, Blue = DAPI. Scale bar = 20 μm.

651

652   **Figure 7**. High glucose media concentrations reversibly inhibit embryo cavitation. (A) Percent

653   cavitation of blastocysts after 24h culture in each treatment group, indicated by the formation of

654   any cavity in the embryo (n=4, mean ± SEM, p=0.0052 1W-ANOVA). (B) Bright field

655   microscopy images of embryos after 24h treatment in 30 mM D-glucose, followed by recovery

656   in low glucose KSOM for 18 hours. Arrows in the left panel indicate examples of embryos

657   classified as non-cavitated. Thirteen of sixteen non-cavitated embryos after high glucose

658   treatment cavitated after 18 hours of recovery. (C) Blastocyst cell number after 24h culture in

659   each treatment group (n=19-21 per group, mean ± SEM, p=0.5099 1W-ANOVA).

660

661   **Figure 8**. High glucose media concentrations do not significantly change relative p66Shc mRNA

662   and protein abundance in blastocysts. (A) qRT-PCR was performed on pools of 10 blastocysts

663   for relative p66Shc transcript abundance, normalized to levels of exogenously added luciferase

664   (n=3, mean ± SEM, p=0.3783 1W-ANOVA). (B) Immunoblotting was performed on pools of 30

665   blastocysts per treatment group for total p66Shc protein abundance, normalized to levels of β-

666   actin. A representative blot is shown (n=3, mean ± SEM, p=0.5549 1W-ANOVA). (C)

667   Representative immunofluorescence and confocal microscopy images of blastocysts cultured in

668   30 mM D-glucose (right panel) and KSOM only (left panel) for total p66Shc reactivity. Green =

669   p66Shc, Blue =DNA. Scale bar = 20 μm.

670

671   **Figure 9**. Increased p66Shc expression correlates with decreased ATP and increased superoxide

672   in cultured blastocysts. (A) Total ATP content was quantified from pools of 5 blastocysts in each

673   treatment group and normalized to blastocyst cell number. ATP content per cell significantly

674   decreases in blastocysts cultured in low oxygen for 96h compared to in vivo controls (n=3, mean

675   ± SEM, p=0.0.0199 1W-ANOVA). Mean cell numbers for each treatment group are: in vivo =

676   27.43 ± 10.31 (n=46), low oxygen = 35.03 ± 7.36 (n=31), high oxygen = 31.41 ± 9.49 (n=30).

677   (B) MitoSOX relative fluorescence was quantified in blastocysts in each treatment group.

678   MitoSOX fluorescence significantly increases in blastocysts cultured under low or high oxygen

679   compared to in vivo controls (in vivo n=28, low oxygen n=26, high oxygen n=23, mean ± SEM,

680   p<0.0001 1W-ANOVA). Representative images of MitoSOX staining are shown in the three

681   panels.

682

683   **Supplemental Figure 1**. NT-Shc and phosphorylated S36 p66Shc antibody validation for

684   immunofluorescence and confocal microscopy. (A) Immunofluorescence and confocal

685   microscopy images of p66Shc-HA transfected HT-22 cells (left) and non-transfected cells

686   (right). Green = total p66Shc, Red = HA, Blue = DAPI. Scale bar = 50 μm. (B) Images of

687   p66Shc-HA transfected HT-22 cells (left) and non-transfected cells (right). Green = pSer36-

688   p66Shc, Red = HA, Blue = DAPI. Scale bar = 50 μm.

689

690   **Supplemental Figure 2**. Relative p66Shc mRNA and protein abundance in cultured 2-cell and

691   8-cell embryos. (A) qRT-PCR was performed on pools of 20 2-cell embryos for p66Shc relative

692   transcript abundance. P66Shc transcript abundance significantly decreases with culture and

693   increasing oxygen tension (n=4, mean ± SEM, p=0.0310 1W-ANOVA). Immunoblotting was

694   performed on pools of 50 2-cell embryos for p66Shc relative protein abundance. A representative

695   blot is shown (n=3, mean ± SEM, p=0.7256 1W-ANOVA). (B) qRT-PCR was performed on

696   pools of 20 8-cell embryos for p66Shc relative transcript abundance, which significantly

697   decreases with culture and increasing oxygen tension (n=4, mean ± SEM, p=0.0004 1W-

698   ANOVA). Immunoblotting was performed on pools of 50 8-cell embryos for p66Shc relative

699   protein abundance. A representative blot is shown (n=4, mean ± SEM, p=0.8375 1W-ANOVA).

700

Table I. Oligonucleotide Primer Sequences		Expected product size
p66Shc R (reverse transcription)	5'-GGTGGATTCCTGAGATACTGTTT-3'	N/A
p66Shc (qPCR)	F: 5'-CCGACTACCCTGTGTTCCTTCTT-3' R: 5'-CCCATCTTCAGCAGCCTTTCC-3'	111 bp
Ppia	F: 5'-GTCCTGGCATCTTGTCCATG-3' R: 5'-TGCCTTCTTTCACCTTCCCA-3'	126 bp
H2afz	F: 5'-CGCAGAGGTACTTGAGTTGG-3' R: 5'-TCTTCCCGATCAGCGATTTG-3'	176 bp
Luciferase	F: 5'-TTGACAAGGATGGATGGCTAC-3' R: 5'-TTCGGTACTTCGTCCACCAAAC-3'	336 bp
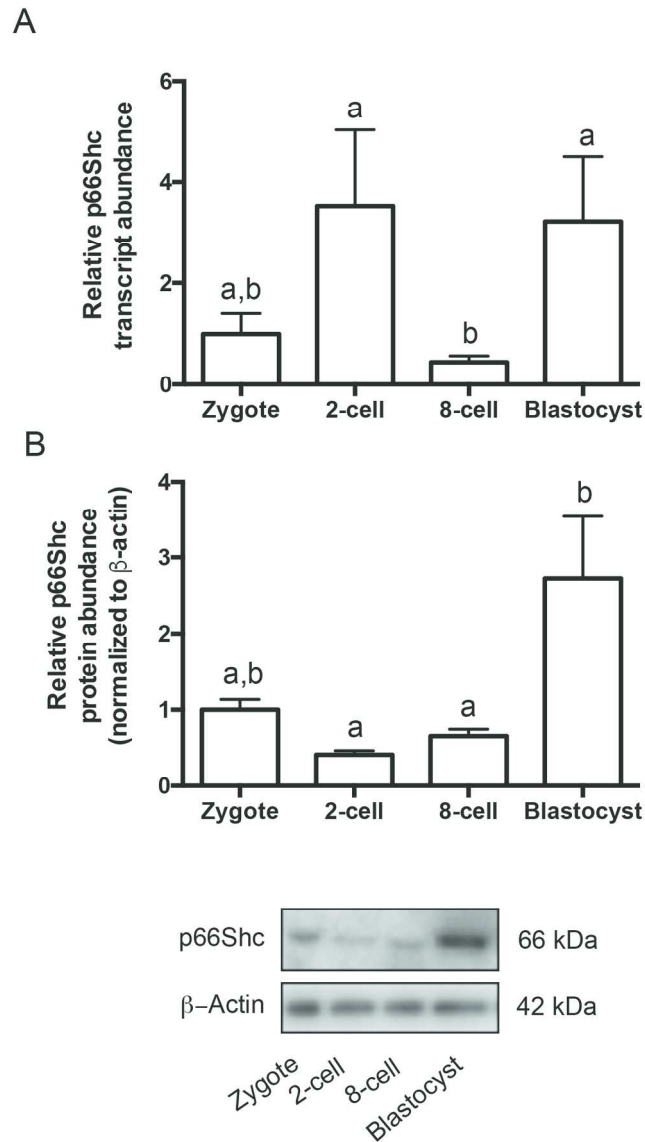
Figure 1. p66Shc expression increases during mouse preimplantation development in vivo. (A) RT-qPCR for p66Shc relative transcript abundance was performed on three replicates of pools of 20 embryos per stage. P66Shc relative transcript abundance significantly increases from eight cell to blastocyst-stage embryos (n=3, mean SEM, p=0.0476 1W-ANOVA). (B) Immunoblotting for total p66Shc protein abundance was performed on three replicates of pools of 30-50 embryos per stage. P66Shc relative protein abundance increases from eight cell to blastocyst-stage embryos (n=3, mean SEM, p=0.0331 1W-ANOVA). A representative blot is shown.

129x199mm (300 x 300 DPI)
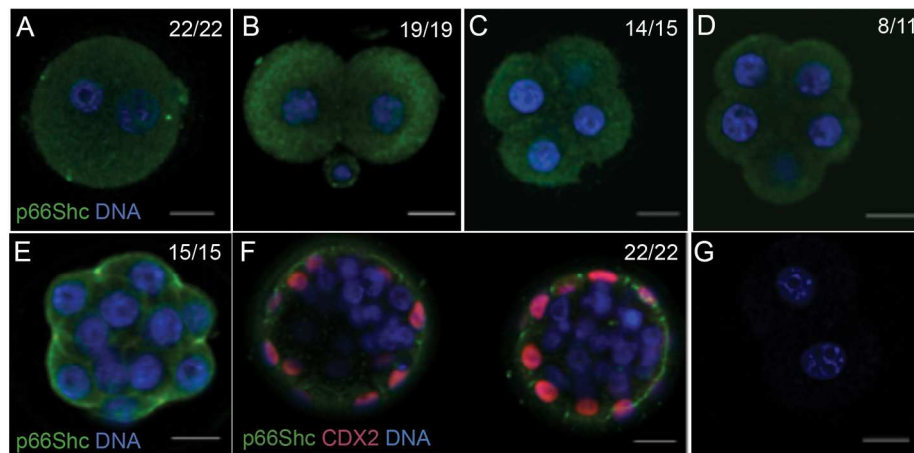
Figure 2. p66Shc progressively localizes to the cell periphery during mouse preimplantation development. Immunofluorescence and confocal microscopy for p66Shc was performed on 10-20 embryos per stage. Representative confocal images are shown: (A) Zygote (B) 2-cell embryo (C) 4-cell embryo (D) 8-cell non-compacted embryo (E) 8-16 cell compacted morula (F) Blastocyst, counterstained for CDX2 (G) Primary antibody omitted. Green = p66Shc, Red = CDX2, Blue = DAPI. Scale bar = 20 m.
180x82mm (300 x 300 DPI)
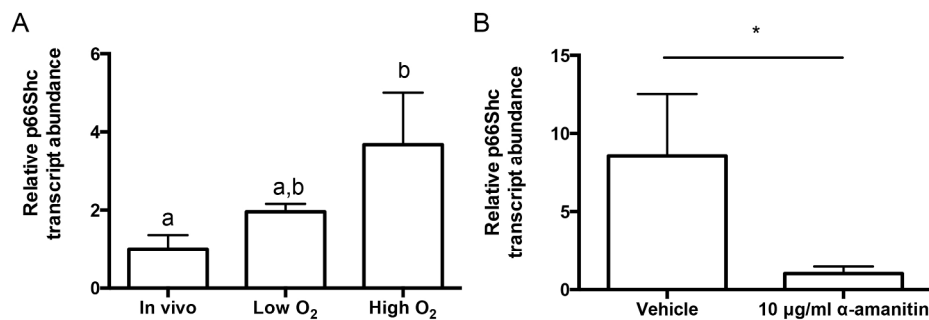
A

B

Figure 3. Culture and high oxygen tension increases the relative p66Shc mRNA abundance in blastocysts. (A) RT-qPCR for p66Shc was performed on four replicates of pools of 20 blastocysts. There is a significant increase in p66Shc mRNA abundance in blastocysts cultured at high oxygen tension compared to in vivo controls (n=4, mean SEM, p=0.0305 1W-ANOVA). (B) Blastocysts cultured for 24h in 10 g/ml -amanitin showed significantly decreased p66Shc transcript abundance compared to controls (n=3, mean SEM, p=0.0477 Student's t-test).
215x80mm (300 x 300 DPI)
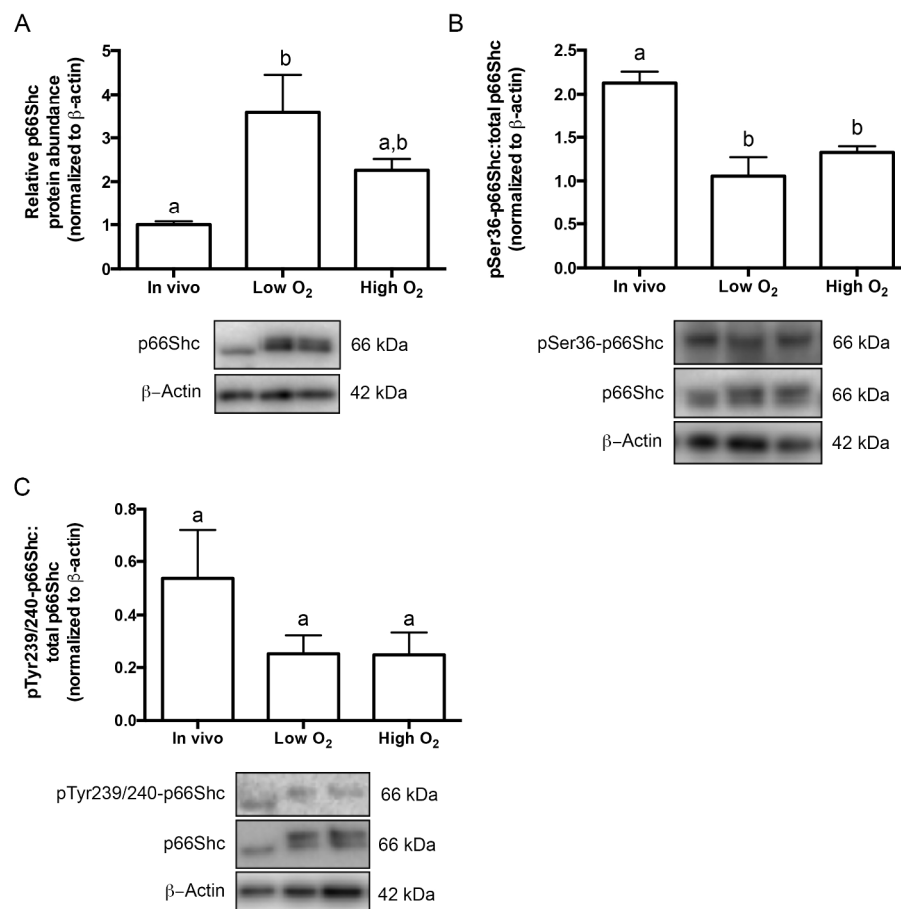
Figure 4. Culture and high oxygen tension increases the relative p66Shc protein abundance in blastocysts. (A) Immunoblotting for p66Shc was performed on four replicates of pools of 50 blastocysts. P66Shc protein abundance significantly increases in blastocysts cultured at low oxygen tension compared to in vivo controls (n=4, mean SEM, p=0.0306 1W-ANOVA). A representative blot is shown. (B) Immunoblotting for phosphorylated p66Shc on serine 36 (S36) and total p66Shc was performed on three replicates of pools of 40-50 blastocysts. The ratio of phospho (S36)-p66Shc:total p66Shc significantly decreases in cultured blastocysts compared to controls (n=3, mean SEM, p=0.0057 for low O2; p=0.0219 for high O2 1W-ANOVA). A representative blot is shown. (C) Immunoblotting for phosphorylated Y239/Y240-p66Shc and total p66Shc was performed on three replicates of pools of 20-30 blastocysts. The ratio of phosphor Y239/Y240-p66Shc:total p66Shc does not significantly in cultured blastocysts compared to controls (n=3, mean SEM, p=0.5043, 1W-ANOVA). A representative blot is shown.
215x279mm (300 x 300 DPI)
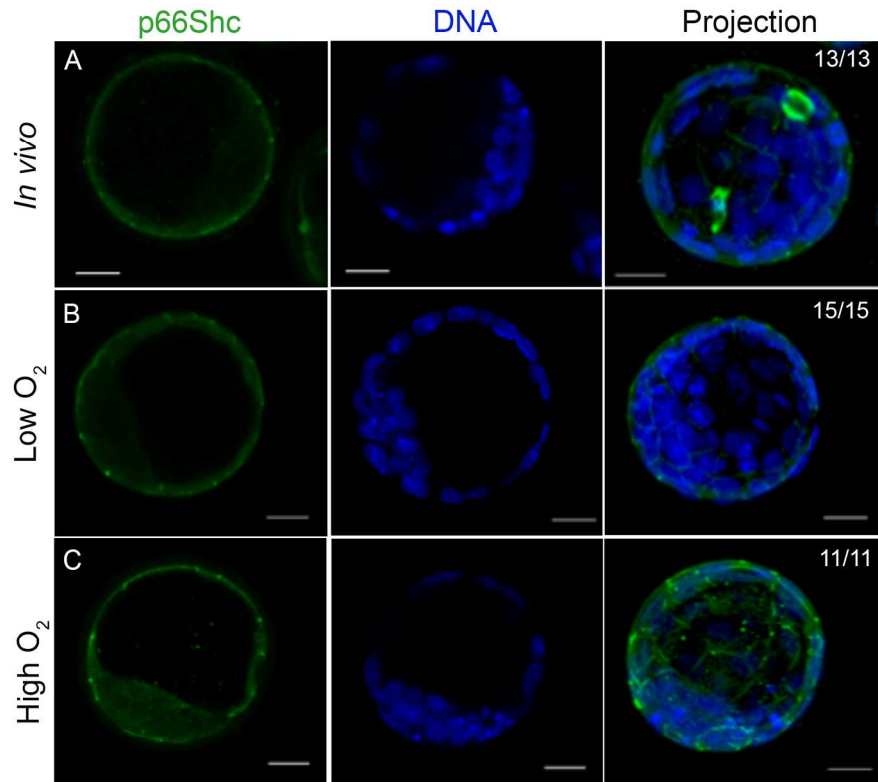
Figure 5. Total p66Shc becomes detectable in the inner cells of blastocysts cultured under atmospheric oxygen tension. Representative immunofluorescence and confocal microscopy images for total p66Shc in pools of 10-15 blastocysts per treatment group. (A) In vivo flushed blastocysts. (B) Blastocysts after 96 h culture under low oxygen tension. (C) Blastocysts after 96 h culture under high oxygen tension. Green = p66Shc, Blue = DAPI. Scale bar = 20 μm.
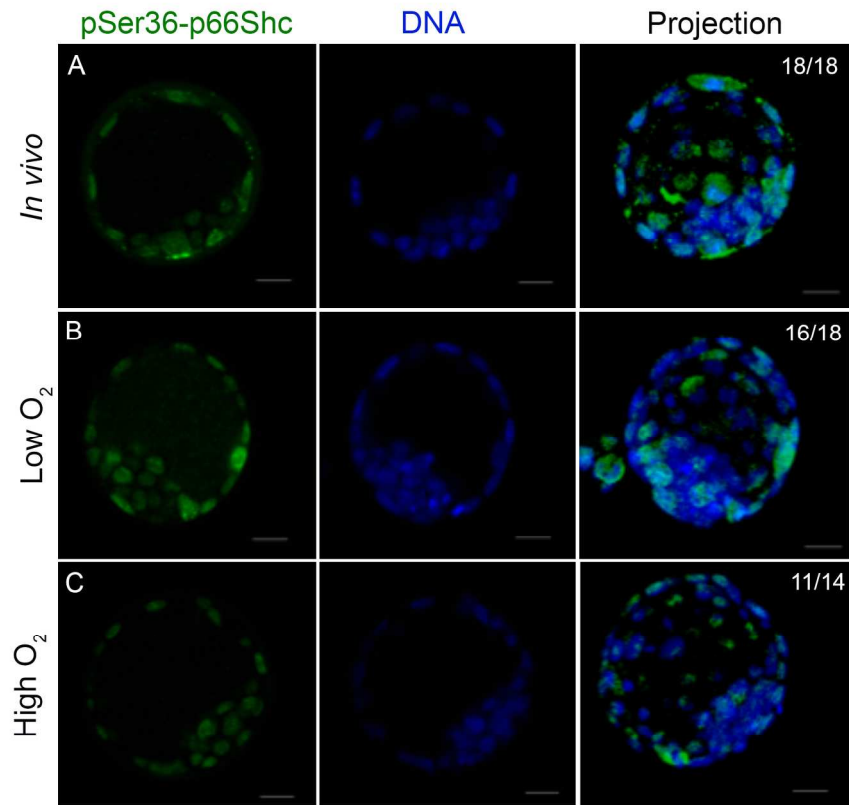184x165mm (300 x 300 DPI)

Figure 6. Phosphorylated S36 p66Shc localization does not change in cultured blastocysts. Representative immunofluorescence and confocal microscopy images for phosporylated (S36) p66Shc in pools of 15-20 blastocysts per treatment group. (A) In vivo flushed blastocystμs. (B) Blastocysts after 96 h culture under low oxygen tension. (C) Blastocysts after 96 h culture under high oxygen tension. Green = p66Shc, Blue = DAPI. Scale bar = 20 m.
184x165mm (300 x 300 DPI)
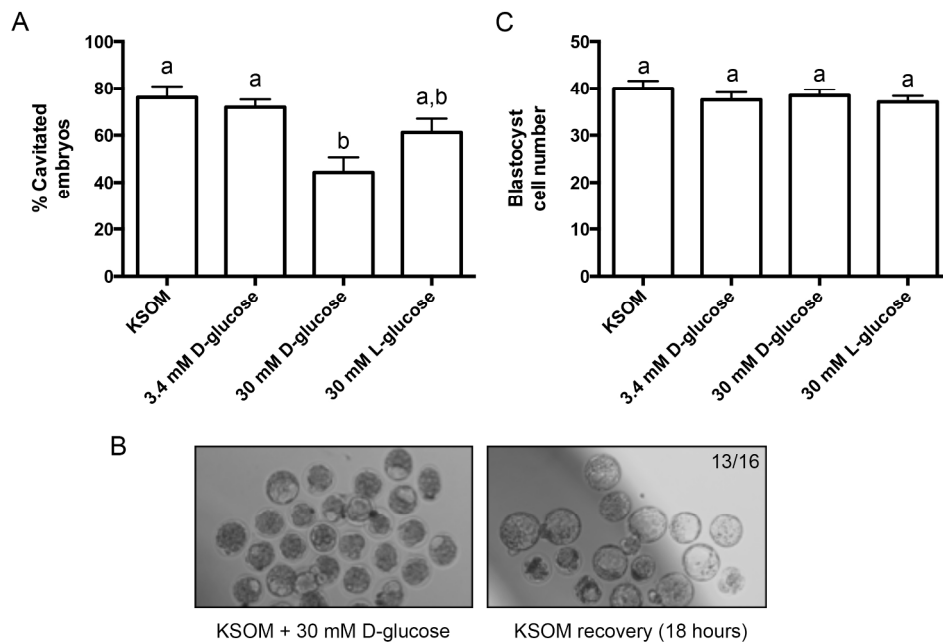
Figure 7. High glucose media concentrations reversibly inhibit embryo cavitation. (A) Percent cavitation of blastocysts after 24h culture in each treatment group, indicated by the formation of any cavity in the embryo (n=4, mean SEM, p=0.0052 1W-ANOVA). (B) Bright field microscopy images of embryos after 24h treatment in 30 mM D-glucose, followed by recovery in low glucose KSOM for 18 hours. Arrows in the left panel indicate examples of embryos classified as non-cavitated. Thirteen of sixteen non-cavitated embryos after high glucose treatment cavitated after 18 hours of recovery. (C) Blastocyst cell number after 24h culture in each treatment group (n=19-21 per group, mean ±SEM, p=0.5099 1W-ANOVA).
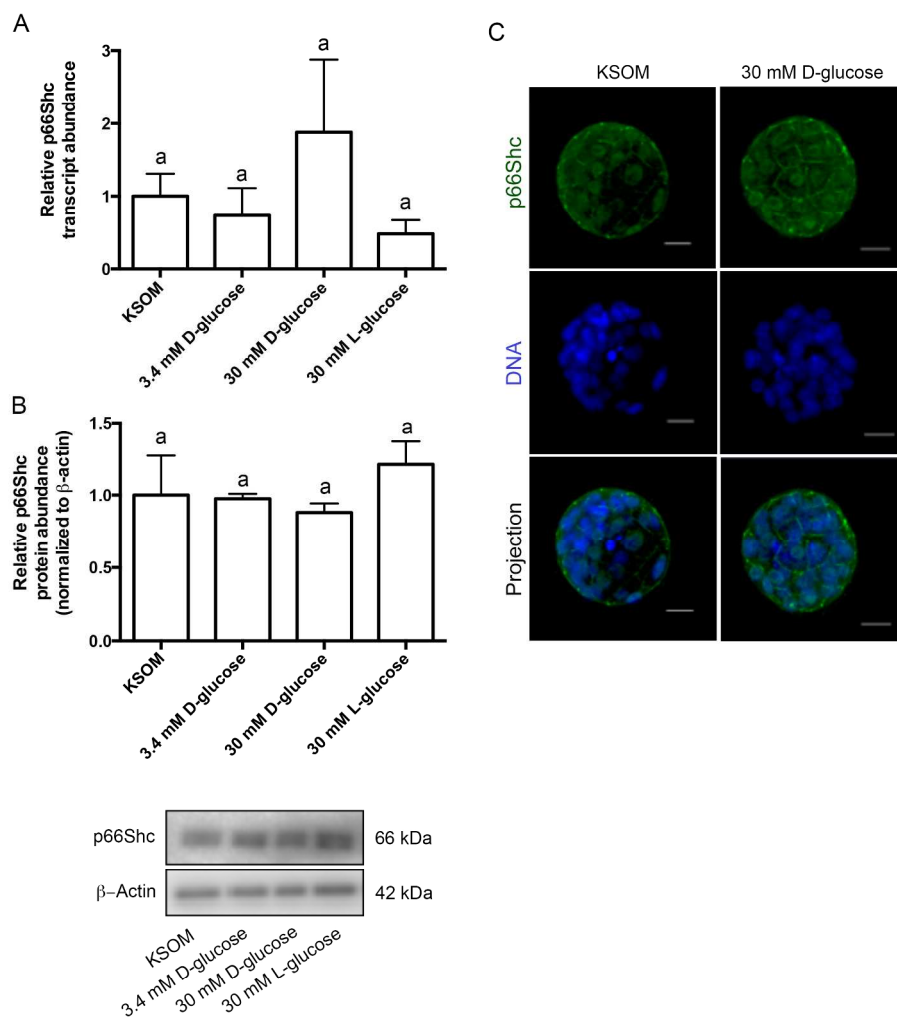215x160mm (300 x 300 DPI)

Figure 8. High glucose media concentrations do not significantly change relative p66Shc mRNA and protein abundance in blastocysts. (A) qRT-PCR was performed on pools of 10 blastocysts for relative p66Shc transcript abundance, normalized to levels of exogenously added luciferase (n=3, mean SEM, p=0.3783 1W-ANOVA). (B) Immunoblotting was performed on pools of 30 blastocysts per treatment group for total p66Shc protein abundance, normalized to levels of β-actin. A representative blot is shown (n=3, mean ±SEM, p=0.5549 1W-ANOVA). (C) Representative immunofluorescence and confocal microscopy images of blastocysts cultured in 30 mM D-glucose (right panel) and KSOM only (left panel) for total p66Shc reactivity. Green = p66Shc, Blue =DNA. Scale bar = 20 μm.
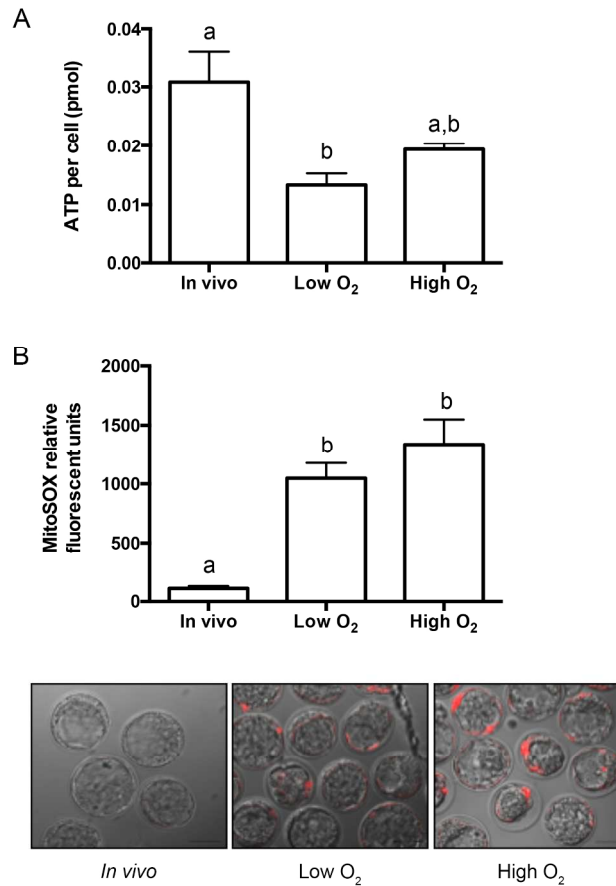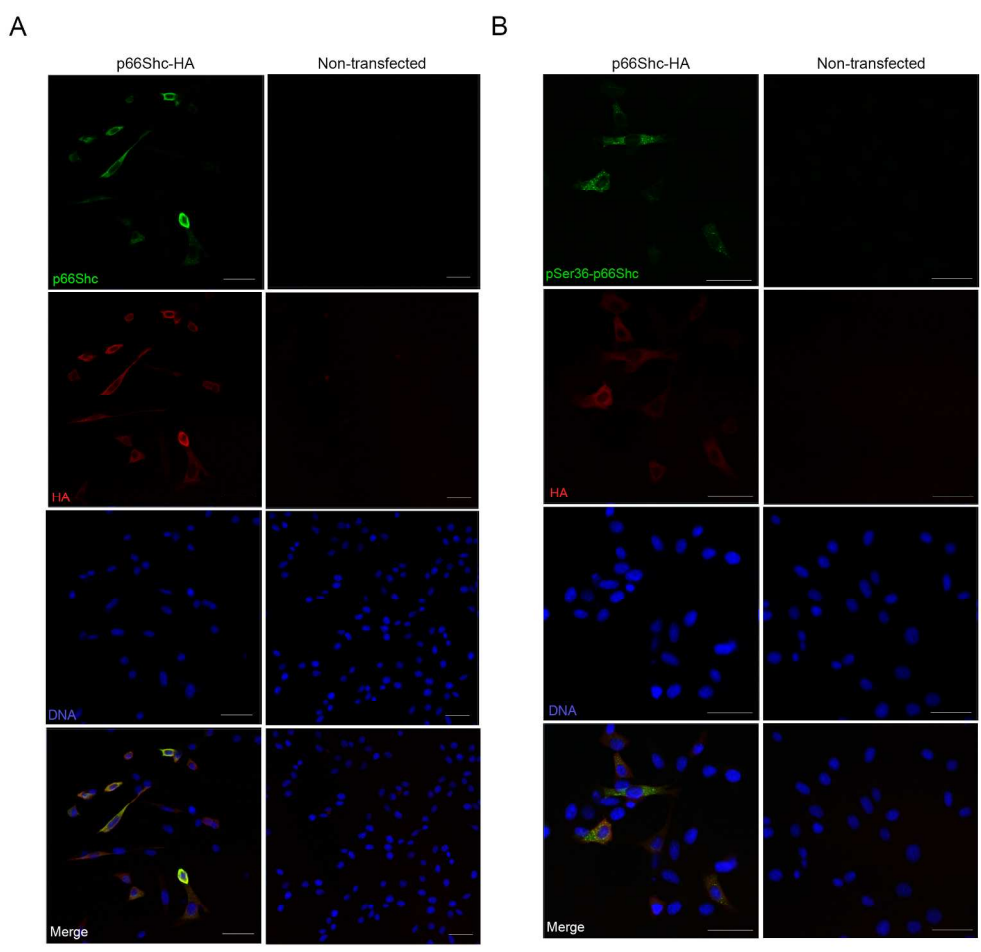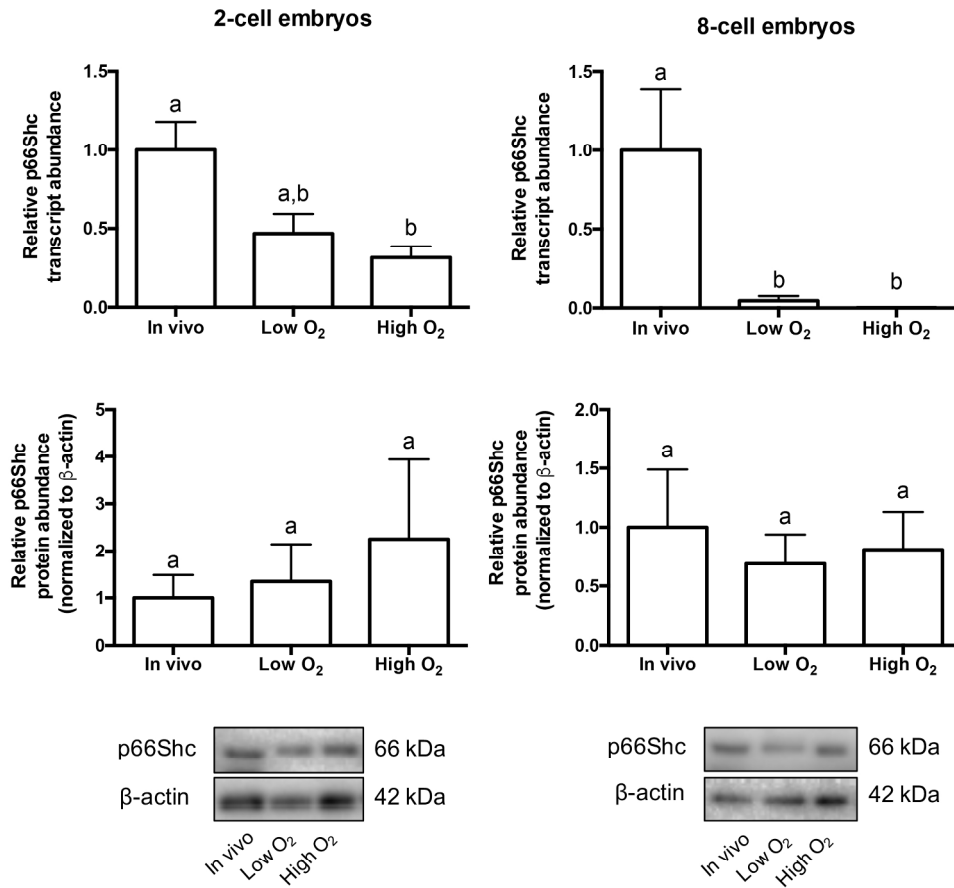215x279mm (300 x 300 DPI)

Figure 9. Increased p66Shc expression correlates with decreased ATP and increased superoxide in cultured blastocysts. (A) Total ATP content was quantified from pools of 5 blastocysts in each treatment group and normalized to blastocyst cell number. ATP content per cell significantly decreases in blastocysts cultured in low oxygen for 96h compared to i*n vivo* controls (n=3, mean ±SEM, p=0.0.0199 1W-ANOVA). Mean cell numbers for each treatment group are: in vivo = 27.43 10.31 (n=46), low oxygen = 35.03 7.36 (n=31), high oxygen = 31.41 9.49 (n=30). (B) MitoSOX relative fluorescence was quantified in blastocysts in each treatment group. MitoSOX fluorescence significantly increases in blastocysts cultured under low or high oxygen compared to *in vivo* controls (*in vivo* n=28, low oxygen n=26, high oxygen n=23, mean ±SEM, p<0.0001 1W-ANOVA). Representative images of MitoSOX staining are shown in the three panels. 215x219mm (300 x 300 DPI)

215x219mm (300 x 300 DPI)

2-cell embryos

8-cell embryos

215x219mm (300 x 300 DPI)